

From Synthetic to Real: Unveiling the Power of Synthetic Data for Video Person Re-ID

Xiangqun Zhang, Ruize Han, Wei Feng
Tianjin University, China

{clzxq, han_ruize}@tju.edu.cn, wfeng@ieee.org

Abstract

In this paper, we study a new problem of cross-domain video based person re-identification (Re-ID). Specifically, we take the synthetic video dataset as the source domain for training and use the real-world videos for testing, which significantly reduces the dependence on real training data collection and annotation. To unveil the power of synthetic data for video person Re-ID, we first propose a self-supervised domain invariant feature learning strategy for both static and temporal features. Then, to further improve the person identification ability in the target domain, we develop a mean-teacher scheme with the self-supervised ID consistency loss. Experimental results on four real datasets verify the rationality of cross-synthetic-real domain adaptation and the effectiveness of our method. We are also surprised to find that the synthetic data performs even better than the real data in the cross-domain setting.

1. Introduction

Person re-identification (Re-ID) is a classical problem in computer vision, which has been developed rapidly in recent years. As a fundamental task, person Re-ID has many real-world applications, such as video surveillance, criminal investigation, etc.

We first review the development of person Re-ID. On one hand, in terms of the data format, early works mainly use a single image for retrieving the specific person [16, 37]. Later, the sequential video data are applied to person Re-ID since it contains more plentiful information [4, 21, 31], e.g., the human gait. On the other hand, in terms of the dataset conditions, early works focus on developing the algorithms on specific dataset by splitting it into the training and testing datasets. This way, the data distributions in the training and testing datasets are similar. In the recent works, unsupervised domain-adaptive (UDA) person Re-ID is proposed aiming to train the model on source domain and test it on the target domain. This is more practical since the characteristics of data in the training and testing sets are al-

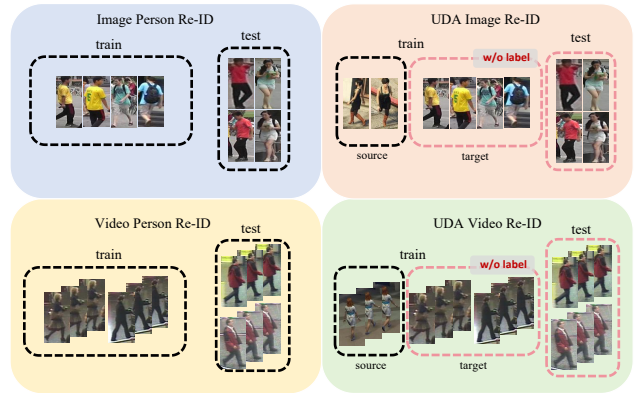


Figure 1. Illustration of different settings for person Re-ID tasks, including the (single domain) image/video person Re-ID and unsupervised domain adaptive (UDA) image/video person Re-ID in previous works. In this work, we focus on a new task of video based UDA person Re-ID. Specifically, we are interested in the scene using the synthetic videos as the source domain, which is more economical and practical.

ways various in the real-world application, including the illumination, viewpoint, etc. For UDA person Re-ID, several works [22, 34] apply the synthetic data for model training to alleviate the burden from data collection and annotation.

Based on the above investigation, we find that the research on cross-domain person Re-ID predominantly focuses on image-based methods, while the exploration of domain adaptive person re-identification for videos is limited, not to mention using synthetic data as the training data. Hence, there is an urgent need to leverage richer temporal videos for synthetic-data based cross-domain person Re-ID. This way, in this work, we aim to utilize large-scale synthetic datasets specifically designed for video-based person Re-ID, to address the challenges of annotating and constructing huge video dataset in real-world scenarios. By leveraging synthetic data, one can learn robust person representations that are invariant to domain variations, leading to significant improvements in the applicability of video-based Re-ID. However, the synthetic-data based cross-domain

video Re-ID brings new challenges. The first one is how to learn the domain-invariant features from the synthetic videos. Second, learning a stable and robust Re-ID model applied to the real data is important yet challenging.

To address these two difficulties, we design the cross-synthetic-real video person Re-ID framework. Specifically, we first design a domain-invariant feature learning module. By integrating three self-supervised auxiliary tasks, this module learns the domain-invariant feature for both single frame and whole sequences. Next, we apply the mean-teacher scheme to improve the model reliability trained on synthetic data for applying to the real data. This scheme includes a teacher network containing the history information, that can be adopted to backward “supervise” the training of the main model, namely student network. We specifically design the consistency loss between the teacher and student networks in a self-supervised manner.

The main contributions of this work are listed as follows.

- We explore a new problem of cross-domain video person Re-ID with synthetic data. We have built the benchmark for this problem, including the training, evaluation datasets and comparative methods.
- We develop a new method for this problem. The proposed model can learn the domain-invariant feature from the synthetic and real domains, and be effectively applied to the real data evaluation, both of which are achieved through the designed self-supervised losses.
- Extensive experimental results demonstrate the effectiveness of the proposed method, which outperforms the comparative methods over 5.8%, 3.5%, 11.7%, and 5.6% on four evaluation datasets. Further analysis also verifies that the utilization of synthetic videos for cross-domain video person Re-ID is effective, even better than real videos.

2. Related Work

Video-based person Re-ID is different from image-based Re-ID, which relies on videos as input and contains richer spatial-temporal information compared to static images. Therefore, exploring spatial-temporal cues is crucial in video-based person Re-ID problem. With respect to the stable spatial representation, the method in [8] builds the appearance-preserving module to solve the problem of appearance destruction. Another work [1] combines salient-to-broad attention and interaction-driven message passing to capture spatial information. Specific for the challenge of changing clothes, CCVID [9] proposes a clothes-based adversarial loss to mine clothes-irrelevant features for clothes-changing video person Re-ID. Similarly, to obtain more effective temporal representations, many technologies are developed, such as complementary features of successive frames [12], temporal reciprocal learning for temporal information accumulation [20], and temporal shift attention module [27]. Furthermore, some approaches focus on ag-

gregating both spatial and temporal features to address spatial and temporal distractors. A spatial-temporal aggregation module is proposed to enhance the aggregation capability [25]. Another work [7] leverages spatial-temporal memories to refine frame-level person representations to get sequence-level representation. The axial-attention strategy is utilized to capture spatial and temporal relations for addressing the misalignment issue in video-based Re-ID [19]. These methods aim to fuse features from multiple temporal and spatial scales to obtain comprehensive representations. We find that although significant progress has been made in *video person Re-ID*, in which *cross-domain scenarios has been relatively limited explored*, not to mention that across the synthetic and real domains.

Unsupervised domain-adaptive (UDA) person Re-ID relies on transferring knowledge learned from the source domain to the target domain. First, some approaches enhance the accuracy of representation learning in the target domain by improving clustering methods. The method in [36] utilizes online clustering and label optimization to improve the accuracy of representation learning in target domain. Another work [13] considers the multi-camera distribution and temporal continuity in re-ID to effectively reduce clustering errors. A density-based clustering with adaptive sample augmentation and discriminative feature learning is utilized to estimate and augment person clusters in target domains [33]. Zheng et al. [39] dynamically and progressively update the pseudo labels based on a hierarchical cluster dynamics. Second, some methods focus on generating and refining pseudo-labels to mitigate the impact of label noise in target domain. Wu et al. [28] proposes a multi-centroid memory module that captures different ID information within a cluster. Han et al. [10] proposes a probabilistic uncertainty guided progressive label refinement approach. The work in [17] utilizes a mean teacher model for online label refining. Cho et al. [6] leverages both global and local context information to mitigate label noise. Third, some methods reduce the domain offset between the source domain and the target domain by domain distribution alignment, e.g., the graph convolutional network based multi-domain information fusion module [2], and feature spaces constructing and alignment with the soft labels [32]. The advancements in UDA methods have significantly contributed to for cross-domain person Re-ID. However, these methods predominantly focus on *image-based tasks and have not yet explored video-based tasks*. Differently, this work tackle the challenging task of cross-domain Re-ID in the context of video data, aiming to learn robust and invariant person representations during the temporal variations.

Person Re-ID with synthetic data. In recent years, the difficulty of labeling real data has made synthetic data shine in the field of person Re-ID. Bak et al. [3] propose to synthesize realistic images and minimizing the domain shift be-

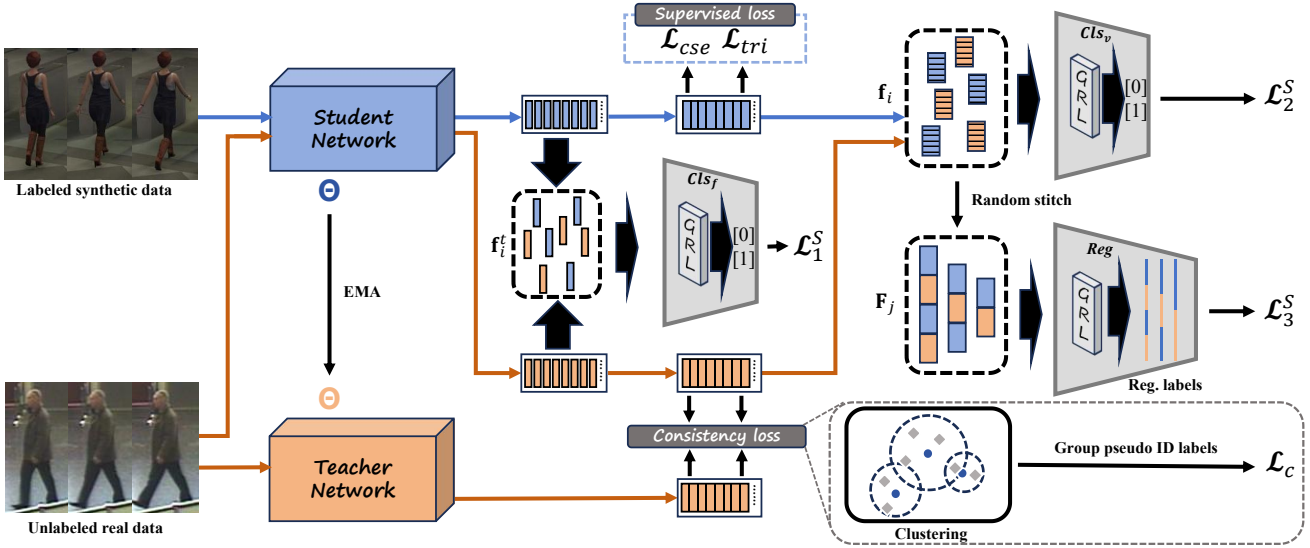


Figure 2. Framework of the proposed method. We use the synthetic videos with ID labels (source domain) and the real videos (target domain) without annotation as input. The main network is trained using the supervised losses on the source domain data. Also, for video representation learning on the domain-mixed data, we design a series of self-supervised losses \mathcal{L}^S to distinguish the domain labels under different levels, including frame, video and combined video. We further apply a mean-teacher strategy for the network training on the unlabeled real data. By taking the main network as student, we use the EMA to obtain a teacher network to “supervise” it, which is achieved by the self-supervised consistency loss \mathcal{L}^C between them.

tween synthetic and real images. Later, a number of large-scale image-based synthetic datasets [22, 26, 34] have been proposed for person Re-ID, which provide realistic appearance and clothing by generating virtual human models as a cost-effective alternative to collecting and labeling real data. A series of methods [14, 29, 30] for cross-domain person Re-ID have demonstrated the effectiveness of cross-domain design from synthetic to real. A recent work [23] presents a large-scale video-based synthetic person Re-ID dataset that demonstrates the potential of synthetic data for person Re-ID in challenging scenarios. As discussed above, researches on *synthetic data based person Re-ID mainly focus on image-based tasks, the exploration of which using video data is limited and worth studying.*

3. Proposed Method

3.1. Problem formulation

We first formulate the unsupervised domain adaptive (UDA) video-based person Re-ID problem. As the classical UDA problem, we use the videos in the source domain with ID labels

$$\mathcal{V}^L = \{(x_i, y_i) | i = 1, \dots, N_L\}, \quad (1)$$

where N_L denotes the number of video sequences. For i -th sequence x_i^L in the source domain dataset, we can obtain the corresponding person ID label $y_i \in \{1, 2, \dots, C^L\}$, where C^L is the number of whole person IDs. We also use the

unlabeled videos in the target domain

$$\mathcal{V}^U = \{(u_j) | j = 1, \dots, N_U\}, \quad (2)$$

as input, where N_U represents the number of sequences in the target domain dataset, but the identity label of each sequence u_j is unavailable. With the above training data, we aim to estimate the ID of each sequence μ_k in the testing dataset

$$\mathcal{V}^T = \{(\mu_k) | k = 1, \dots, N_T\}. \quad (3)$$

In this work, we specifically study the UDA problem from the synthetic data to the real data. This way, we use the synthetic videos as the source domain \mathcal{V}^L , and the real-world videos are used as the unlabeled training set \mathcal{V}^U and testing set \mathcal{V}^T .

3.2. Domain invariant feature learning

Basic feature extraction. Given the videos \mathcal{V}^L in the source domain, we first apply an existing deep learning model for video Re-ID feature extraction, e.g., SINet [1], as the backbone

$$f_i = F(x_i | \Theta), \quad p_i = \phi(f_i), \quad (4)$$

where $F(\cdot | \Theta)$ denotes the feature extraction function with the parameters Θ . f_i is the extracted feature of the video sample x_i . After that, we use the classifier function $\phi(\cdot)$, that is composed of the FC layers with the ‘softmax’ activation function, to map the feature into the ID prediction

vector $\mathbf{p}_i \in \mathbb{R}^C$. The probabilities of x_i belonging to all C^L identities is provided by \mathbf{p}_i .

Supervised loss. Given the person ID label y_i in the source domain, we can train the above models F and φ using the supervised manner. Specifically, we minimize the discrepancy between predicted and the ground-truth ID results. We first denote a one-hot vector \mathbf{y}_i with $\mathbf{y}_i(c) = 1$ if the index c equals to the correct ID label y_i , otherwise $\mathbf{y}_i(c) = 0$. We apply two classical losses, i.e., the cross-entropy loss and the triplet loss as below

$$\mathcal{L}_{\text{cse}} = - \sum_c \mathbf{y}_i(c) \log \mathbf{p}_i(c), \quad (5)$$

$$\mathcal{L}_{\text{tri}} = [D(\mathbf{f}_a, \mathbf{f}_p) - D(\mathbf{f}_a, \mathbf{f}_n) + m]_+, \quad (6)$$

where $\mathbf{f}_a, \mathbf{f}_p, \mathbf{f}_n$ denote the feature of the anchor, positive, and negative sample, respectively. We use $D(\cdot, \cdot)$ to measure the Euclidean distance between the two feature vectors, and m is the margin of used in triplet loss.

Self-supervised loss for domain discrimination. Inspired by recent advancements in self-supervised learning, besides the above supervised Re-ID loss, we also employ self-supervised domain-adaptive loss to reduce cross-domain differences, for which we design the self-supervised auxiliary tasks without external annotations. Specifically, we focus on simultaneously addressing cross-domain and temporal feature learning. We aim to achieve effective cross-domain video person Re-ID and learn pedestrian features that are invariant to domain difference and temporal variations. For this purpose, we develop a simple and effective strategy by integrating two self-supervised auxiliary tasks for domain discrimination, as shown in Fig. 2.

We use both the videos \mathcal{V}^L in source domain and the videos \mathcal{V}^U in the target domain together. We first get the frame-level feature \mathbf{f}_i^t of sequence x_i or u_j , which denotes the feature of one frame at time t . Then, we apply a binary domain prediction task to predict the domain of each frame-level feature

$$d_i^t = \text{Cls}_f(\mathbf{f}_i^t), \quad (7)$$

where d_i^t denotes the domain prediction result of \mathbf{f}_i^t , i.e., source domain or target domain. The function Cls_f is a binary classification function. Similarly, we also consider the video-level domain discrimination as

$$d_i = \text{Cls}_v(\mathbf{f}_i), \quad (8)$$

where \mathbf{f}_i denotes the feature of a input sequence, and d_v denotes the binary domain prediction result of video \mathbf{f}_i , and Cls_v also denotes the binary classification. The domain label of each frame or video is easy to obtain, therefore the above training can be conducted in the self-supervised manner. Besides, we further stitch the features from multiple sequences with a random permutation, as shown in Fig. 2.

The number of sequences for combination is arbitrary, e.g., 2,4,8, etc. Then, we aim to predict the domain distribution of the combined features. The prediction can not be achieved by a classification problem, since the number of sequences in each combined features is variable. This way, we design a regression strategy for the domain prediction. Specifically, for S sequence features \mathbf{f}_i , we use the temporal feature aggregation method [5] to form the combined feature as \mathbf{F}_j . Then we predict its domain distribution by

$$d_j^F = \text{Reg}(\mathbf{F}_j), \quad (9)$$

where d_j^F is an one-dimensional vector with fixed length. Given the domain label of S video sequences, we can also get the domain distribution of the combined videos, as shown in Fig. 2.

The total self-supervised loss for domain discrimination is defined as

$$\begin{aligned} \mathcal{L}^S &= \mathcal{L}_1^S + \mathcal{L}_2^S + \mathcal{L}_3^S \\ &= \sum_i \sum_t \mathcal{L}_{\text{cse}}(d_i^t, \tilde{d}_i^t) + \sum_i \mathcal{L}_{\text{cse}}(d_i, \tilde{d}_i) \\ &\quad + \sum_j \mathcal{L}_{\text{mse}}(d_j^F, \tilde{d}_j^F), \end{aligned} \quad (10)$$

where $\tilde{d}_i^t, \tilde{d}_i$ and \tilde{d}_j^F denote the label of d_i^t, d_i and d_j^F , respectively. Here we use the cross-entropy loss \mathcal{L}_{cse} for classification in \mathcal{L}_1^S and \mathcal{L}_2^S , and the MSE loss \mathcal{L}_{mse} for regression in \mathcal{L}_3^S .

Note that, during training, we apply the adversarial training strategy by using a gradient reversal layer (GRL), which reverses the gradient signs during back-propagation. The basic insight is that, with GRL, the domain discrimination ability gets stronger as the cross-domain features consistency increase. This way, the classification will be optimized to gradually align the feature distributions between the two domains. By integrating these two auxiliary tasks, we achieve domain-invariant feature learning across both individual frames and entire video sequences. This enables us to handle the invariant feature learning under cross-domain and over-time variations effectively.

3.3. Consistency learning on unlabeled real data

A mean-teacher scheme. As shown in Fig. 2, we apply the mean-teacher strategy for the learning on unlabeled real data. Specifically, based on the basic network trained with supervised and self-supervised losses as discussed above, we take it as the ‘Student’ S and distill it as the ‘Mean Teacher’ network \mathcal{T}

$$\mathcal{T} = \text{EMA}(S), \quad (11)$$

where $\text{EMA}(\cdot)$ denotes the exponential moving average (EMA) approach. In this scheme, teacher \mathcal{T} contains the

history information of \mathcal{S} , This way, \mathcal{T} can be adopted to backward “supervise” the training of student \mathcal{S} on real data without supervised label. We design the consistency loss between \mathcal{T} and \mathcal{S} for self-supervision.

Self-supervised identification consistency loss. Given the real video sequence u_j in \mathcal{V}^U , we first extract the feature of each video

$$\mathbf{f}_j^{\mathcal{S}} = \mathcal{S}(u_j), \mathbf{f}_j^{\mathcal{T}} = \mathcal{T}(u_j), j = 1, \dots, N_U, \quad (12)$$

where $\mathbf{f}_j^{\mathcal{S}}$ and $\mathbf{f}_j^{\mathcal{T}}$ denotes the feature through the student and teacher networks, respectively. A straightforward idea to estimate the consistency loss between \mathcal{T} and \mathcal{S} is to calculate the distance between $\mathbf{f}_j^{\mathcal{S}}$ and $\mathbf{f}_j^{\mathcal{T}}$. This may lead to the gradient computation issue because of the large feature distance. As discussed in previous works [5], a better manner to estimate the consistency is to use the result of target task rather than the middle features. This way, a plausible approach is to apply the classification based on the features to obtain the person IDs. However, this will run into two problems. First, the number of IDs in dataset \mathcal{V}^U is not provided in prior, i.e., the number classification categories, is unknown. Second, the ID indexes obtained from the classification of \mathcal{T} and \mathcal{S} are unaligned. To address the above problems, we propose a clustering based identification consistency estimation strategy.

We first take all the features $\mathbf{f}_j^{\mathcal{S}}$ and $\mathbf{f}_j^{\mathcal{T}}$ together and apply a clustering algorithm to group these features into M clusters

$$\{C_1, C_2, \dots, C_m\} = \text{Cluster}(\mathbf{f}_j^{\mathcal{S}}, \mathbf{f}_j^{\mathcal{T}}), j = 1, \dots, N_U, \quad (13)$$

where C denotes the cluster, which contain different features. Note that, this process aims to cluster the samples with the same ID into the same group, where cluster index can be regarded as the pseudo ID label. With the clustering result, we first define the ID consistency loss as

$$\mathcal{L}_1^C = \sum_{j=1}^{N_U} \Pi(C\{\mathbf{f}_j^{\mathcal{S}}\}, C\{\mathbf{f}_j^{\mathcal{T}}\}), \quad (14)$$

where $C\{\cdot\}$ denotes the cluster index of $\mathbf{f}_j^{\mathcal{S}}$ or $\mathbf{f}_j^{\mathcal{T}}$ in Eq. (13). $\Pi(a, b)$ is the indicative function, which results 0 when $a = b$, and results 1 when $a \neq b$. This loss constraints that the feature of sample j from \mathcal{T} and \mathcal{S} to be in the same cluster, i.e., with the same pseudo ID. We also use an ID similarity loss as below

$$\mathcal{L}_2^C = \sum_m (d(\bar{\mathbf{f}}_m - \mathbf{f}_j^*) | \mathbf{f}_j^* \in C_m), * = \mathcal{S}, \mathcal{T}, \quad (15)$$

where $\bar{\mathbf{f}}_m$ denotes the mean feature in cluster m , d is a distance function. This loss calculates the feature similarities of all features in the same cluster. Through this loss, we aim

to shorten the distances among the features from \mathcal{S} and \mathcal{T} if they have the same pseudo ID.

Compared to directly computing the feature distance, the above strategy incorporate considerations of the overall data distribution and the relationship information among the samples, which can better constrain the identification consistency. The self-supervised identification consistency loss is defined as

$$\mathcal{L}^C = \mathcal{L}_1^C + \mathcal{L}_2^C, \quad (16)$$

3.4. Implementation details

Training strategy. The total loss of our method is defined with two supervised and three self-supervised losses as

$$\mathcal{L} = \mathcal{L}_{\text{cse}} + \mathcal{L}_{\text{tri}} + \mathcal{L}^S + \mathcal{L}^C, \quad (17)$$

which are controlled by a learnable weight vector to determine the ratio among them. The student network is first trained with the supervised losses $\mathcal{L}_{\text{cse}}, \mathcal{L}_{\text{tri}}$ and the domain discriminative loss \mathcal{L}^S . For the training using mean teacher strategy, the weights of teacher network are initialized with those of student network. The EMA method is used to update the weights of the teacher network in each training iteration. Then, the consistency loss $\mathcal{L}_1^C, \mathcal{L}_2^C$ can be applied.

Network details. We use the backbone in a video-based person Re-ID approach, i.e., SINet, as the feature extraction model $F(\cdot|\Theta)$ in Eq. (4). The supervised learning module employs cross-entropy loss and triplet loss for training in Eqs. (5) and (6), with a margin m set to 0.3 for the triplet loss. In the self-supervised domain discrimination module, both the source domain and target domain videos (\mathcal{V}^L and \mathcal{V}^U) are directly fed into the SINet model. For each video composed of multiple frames, frame-level features are extracted and averaged to obtain video-level features. The domain classifier $\text{Cls}(\cdot)$ consists of a fully connected (FC) layer, a ReLU activation function, and a dropout layer. Specifically, $\text{Cls}_f(\cdot)$ and $\text{Cls}_v(\cdot)$ have the same structure with unshared parameters. During the forward propagation, the input data is computed through the domain classifier to produce the final output features. In the backward propagation, the gradients are reversed through the adversarial gradient reversal layer (GRL).

We use K-means algorithm to partition them into M clusters, where M is set to 16. We use $4 \times$ NVIDIA RTX 2080ti for model training, and apply the Adam [15] algorithm for optimization. During the testing phase, given a query, the trained student network retrieves a ranked list from the gallery.

4. Experimental Results

4.1. Setup

Synthetic video Re-ID dataset. previous work [23] uses the highly realistic video game *Grand Theft Auto (GTA)*

Table 1. Comparison with the state-of-the-art Re-ID methods on four pair of cross-domain datasets, i.e., from the synthetic SVReID to the real datasets including Mars, iLIDS-VID, PRID and CCVID. (%)

Methods	SVReID→Mars				SVReID→iLIDS-VID			
	Rank 1	Rank 5	Rank 10	mAP	Rank 1	Rank 5	Rank 10	mAP
CAViT [27]	13.8	24.9	-	6.5	4.0	7.3	-	6.7
PTSA [25]	34.2	50.2	56.4	20.1	23.7	42.3	52.3	30.5
AP3D [8]	44.7	61.3	66.5	<u>25.0</u>	22.7	39.3	50.0	31.7
TCLNet [12]	42.6	57.7	64.9	22.8	26.7	50.0	61.3	34.9
CAL [9]	43.6	58.3	63.6	23.4	25.3	41.3	51.7	31.7
SINet [1]	42.8	57.6	63.1	23.4	29.3	47.3	63.3	<u>39.8</u>
GLT [36]	38.5	55.3	62.9	24.0	12.0	26.0	34.0	20.0
QAconv [18]	40.7	55.6	62.4	22.7	20.0	38.0	48.0	29.4
Ours	48.1	62.9	68.8	30.8	42.0	68.0	78.7	53.3

Methods	SVReID→PRID				SVReID (w cc)→CCVID			
	Rank 1	Rank 5	Rank 10	mAP	Rank 1	Rank 5	Rank 10	mAP
CAViT [27]	13.5	38.2	-	25.2	61.4	70.0	-	42.5
PTSA [25]	47.9	71.4	80.1	51.8	61.4	74.3	80.0	52.6
TCLNet [12]	65.6	74.5	77.9	57.5	42.8	57.6	63.1	23.4
CAL [9]	51.6	73.0	78.7	55.1	70.7	78.1	81.6	<u>66.8</u>
SINet [1]	53.7	75.3	83.2	63.0	70.7	79.1	83.1	64.1
GLT [36]	33.7	62.9	71.9	48.0	68.2	77.6	80.9	59.1
QAconv [18]	50.6	77.5	84.3	61.8	55.4	70.4	75.3	37.8
AP3D [8]	56.2	80.9	92.1	<u>67.4</u>	52.8	62.6	68.2	43.1
Ours	71.9	87.6	89.9	79.1	78.3	84.3	87.3	72.4

V to construct a large-scale dataset for clothes-changing video person Re-ID. The videos were collected in a surveillance scenario, where 10 monitoring cameras are installed across five different scenes (two cameras per scene). We have noticed that this dataset mainly focuses on the clothes-changing challenge in Re-ID problem, thus the person in which has various (2-37) suits. Based on this dataset, we built a *Synthetic-domain-adaptive Video person Re-ID*, namely SVReID dataset. Specifically, we only consider the non-clothing change scenario. From the training set in [23], we extract a subset by selecting the highest number of sequences for each person without clothing variation. Here we get SVReID including 1,164 sequences from 333 identities. We also consider the clothes-changing problem in some real-world video Re-ID datasets, e.g., CCVID [9]. This way, we further extend SVReID by including the clothes-changing videos. Specifically, based on SVReID, we further select the top-8 highest number of sequences with clothing variations, and get totally 3,187 sequences, which forms SVReID (w cc). Note that, we do not directly use the entire large-scale dataset, since selecting subsets can reduce training time. Also, this work does not focus on the clothes-changing problem, thus we keep the clothing scenario same with the corresponding testing dataset, we can more precisely control the experimental conditions. This prevents the model from excessively focusing on irrelevant

data, and we can compare the performance of different methods under the same scenario.

Real-world benchmark datasets. In this work, we evaluate the effectiveness of our domain-adaptive Re-ID method on four prominent real-world video datasets, i.e., MARS [38], iLIDS-VID [24], PRID-2011 [11], and CCVID [9].

- *MARS* is a large-scale dataset including 1,261 identities and approximately 19,000 video sequences, with an average of 59 frames per sequence.
- *iLIDS-VID* consists of 600 video sequences from 300 unique identities, collected using two cameras, with an average of 70 frames per sequence.
- *PRID-2011*, a smaller dataset, comprises 400 video sequences from 200 identities captured by two cameras, with an average of 108 frames per sequence.
- *CCVID* is a Re-ID dataset CCVID derived from a gait dataset FVG [35]. The characteristic of it is with clothing change setting. CCVID contains 2,856 video sequences from 226 identities, with an average of 2 outfits per person, and an average of 121 frames per sequence.

Evaluation metrics. In the field of person Re-ID, the evaluation protocols commonly employed are the Cumulative Matching Characteristic (CMC) curve metrics, specifically Rank 1/5/10, and the mean average precision (mAP) score.

Comparison methods. Due to limited research on cross-

Table 2. Ablation study of the proposed method. (%)

Methods	SVReID→iLIDS-VID				SVReID (w cc)→CCVID			
	Rank 1	Rank 5	Rank 10	mAP	Rank 1	Rank 5	Rank 10	mAP
Baseline	29.3	47.3	63.3	39.8	70.7	79.1	83.1	64.1
+ \mathcal{L}_1^S	32.7	59.3	73.3	45.4	71.7	78.3	81.8	68.1
+ $\mathcal{L}_1^S + \mathcal{L}_2^S$	34.0	62.7	75.3	47.3	72.9	80.5	83.1	68.2
+ $\mathcal{L}_1^S + \mathcal{L}_2^S + \mathcal{L}_3^S$	36.0	63.3	75.3	49.1	73.9	79.9	84.2	70.1
w/o \mathcal{L}_1^C	39.0	62.7	73.3	50.1	75.2	82.4	86.8	71.8
w/o \mathcal{L}_2^C	39.3	64.0	78.0	51.2	74.6	80.3	83.8	70.0
Ours	42.0	68.0	78.7	53.3	78.3	84.3	87.3	72.4

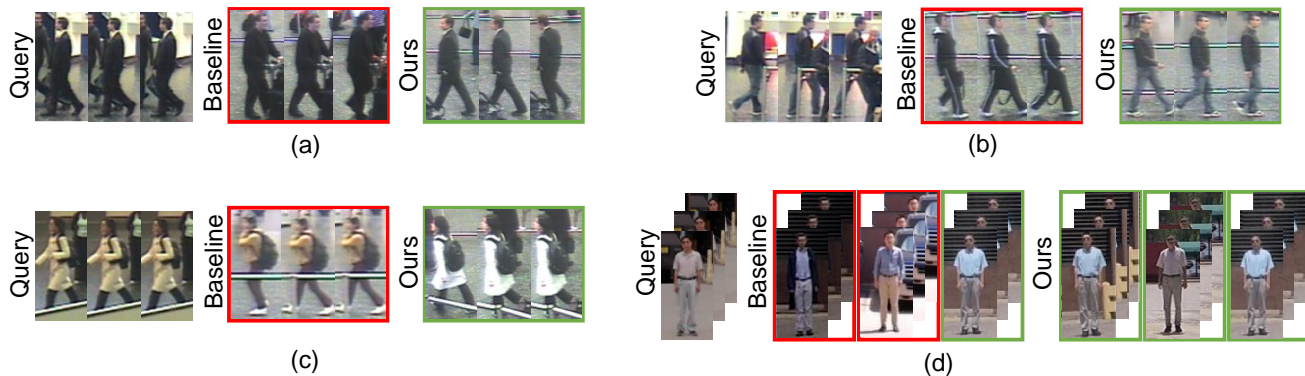


Figure 3. Qualitative analysis of the baseline and the proposed method, under complex background (a), occlusion (b), illumination variation (c) and clothes changing (d).

domain person Re-ID based on videos, we conducted a comprehensive evaluation by comparing our method against two categories of approaches. The first category is the state-of-the-art video-based person Re-ID approaches, including CAViT [27], PSTA [25], AP3D [8], TCLNet [12], SINet [1] and CAL [9]. The second category is image-based person Re-ID methods that aim to handle the unsupervised domain adaptation problem, including GLT [36] and QAconv [18].

4.2. Results

As shown in Tab. 1, we compare our method with the state-of-the-art video person Re-ID approaches and domain adaptive Re-ID approaches. We conduct the experiments on four pairs of cross-domain datasets. We can first see that, the proposed method gets the best performance compared to other approaches with a large margin, on all four real-world datasets. Specifically, we find that our method outperforms the second-best approach over 10% on iLIDS-VID and PRID datasets. The performance improvement on the large-scale Mars dataset also achieves over 5%. On the CCVID dataset, the clothes-changing setting increases the difficulty for Re-ID. In this case, the proposed method still performs better than CAL, which is specifically designed for CCVID to handle the clothes-changing problem. These results demonstrate that the proposed method has an effective domain adaption ability across the synthetic and real-

world scenes.

4.3. Ablation study

To verify the effectiveness of each component in the proposed method, we conduct the ablation study on two datasets, i.e., the medium-scale dataset iLIDS-VID and the clothes-changing aware dataset CCVID, as shown in Tab. 2. First, for the effectiveness of domain-invariant feature learning module, we add the self-supervised domain discrimination losses, i.e., \mathcal{L}_1^S , \mathcal{L}_2^S , and \mathcal{L}_3^S in Eq. (10) one by one. As shown in Tab. 2, we can first see that the proposed self-supervised loss \mathcal{L}^S is effective in improving the Re-ID performance with a large margin. Also, the results demonstrate that each component in \mathcal{L}^S can improve the performance, respectively. With \mathcal{L}^S equipped, we further investigate the effectiveness of the mean-teacher scheme. We find that the integrating of the mean-teacher training strategy can further improve the performance of our method. Also, each sub-loss in \mathcal{L}^C is verified to be useful.

4.4. In-depth analysis

4.4.1 Qualitative analysis

We provide the qualitative results. As shown in Fig. 3, we illustrate the query and the Rank-1 identities of our method and the baseline. From the first case in (a) we can see that our method can effectively handle the complex background

Table 3. Comparison results with the real to real data training. (%)

Methods	Baseline				Ours			
	Rank 1	Rank 5	Rank 10	mAP	Rank 1	Rank 5	Rank 10	mAP
Mars→iLIDS-VID	6.7	12.0	15.3	<u>10.7</u>	8.3	15.7	20.3	<u>14.6</u> (+3.9)
PRID→iLIDS-VID	16.7	29.3	41.3	<u>24.4</u>	24.0	42.7	54.0	<u>33.5</u> (+9.1)
SVReID→iLIDS-VID	29.3	47.3	63.3	<u>39.8</u> (↑ 15.4)	42.0	68.0	78.7	<u>53.3</u> (+13.5) (↑ 19.8)
Mars→CCVID	62.6	75.3	83.3	<u>55.0</u>	70.3	79.1	84.4	<u>60.5</u> (+5.5)
PRID→CCVID	43.6	58.9	64.6	<u>33.9</u>	65.5	80.5	84.4	<u>54.2</u> (+20.3)
SVReID (w cc) →CCVID	70.7	79.1	83.1	<u>64.1</u> (↑ 9.1)	78.3	84.3	87.3	<u>72.4</u> (+8.3) (↑ 11.9)

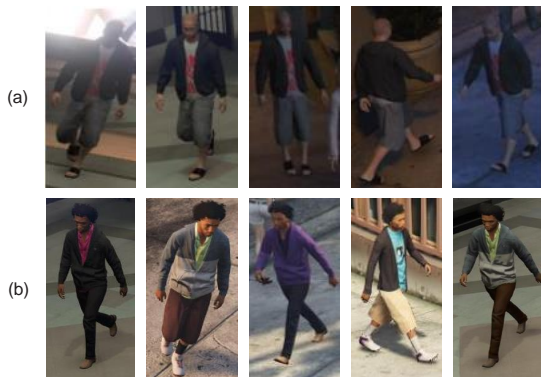


Figure 4. Illustration of some examples in SVReID of the same identity with various styles (a) and clothes changing (b).

around the person. Similarly, from the second case we can also see that our method can handle the occlusions appearing in the query video. The third case demonstrates that our method can deal with the problem of style difference between the query and gallery. Specifically, we find that the baseline method seeks the person heavily depending on the appearance similarity, which is unable when the videos have large style gap, as shown in Fig. 3(c). Our method addresses these problems since it learns more domain-invariant temporal features from the target itself, which is discriminative and little affected by the surroundings or styles. We also provide a sample with cloth-changing from the CCVID in (d). We find that our model trained on SVReID (w cc) can handle the challenging cloth-changing scenarios. Fig. 4 shows some examples in SVReID (w cc) dataset. Note that, the cloth-changing person videos are easy to collect in the synthetic environment but difficult in real world. Therefore, the usage of synthetic data for cloth-changing video person Re-ID is promising.

4.4.2 Comparison with real to real data training

We further analyze the reasonability of using the synthetic data for cross-domain video person Re-ID. Specifically,

we select two real datasets, i.e., the medium-scale dataset iLIDS-VID and the clothes-changing dataset CCVID for testing, and other two real datasets, i.e., Mars (large) and PRID (small) for training. As shown in Tab. 3, we compare the cross-domain Re-ID results using the real data (as discussed above) and our synthetic data (SVReID) for training. The experiments are conducted with the baseline and the proposed method, respectively. We can first see that, compared to the training on real dataset, i.e., Mars and PRID, the using of our synthetic SVReID improves the Re-ID performance on both iLIDS-VID and CCVID datasets, no matter the baseline or our method. Take the mAP score for example, the margin of improvement achieves 15.4% and 9.1% on iLIDS-VID and CCVID, respectively, for the baseline approach. For our method, the improvement is more significant of 19.8% and 11.9%. This effectively demonstrates that *the utilization of synthetic videos for cross-domain person is rational*.

We further compare the results of each row in Tab. 3. We can see that our method outperforms the baseline significantly on each setting of training and testing datasets. This indicates that *the proposed method can improve the cross-domain robustness not only for the scenes from synthetic to real domain, but also those from real to real*.

5. Conclusion

In this work, we have studied a new and valuable problem of cross-domain video person Re-ID with the synthetic data. For this problem, we develop a new framework, including a domain-invariant feature learning module and a mean-teacher network training scheme, both of which are achieved in a self-supervised manner without extra annotations. We have also built the benchmark including the training/evaluation datasets and comparative results, for this problem. In the future, we plan to build a unified large synthetic dataset, including the clothes unaltering/changing, and other scenarios, for more general video person Re-ID training, for which we also consider to use the recently popular generation models.

References

- [1] Shutao Bai, Bingpeng Ma, Hong Chang, Rui Huang, and Xilin Chen. Salient-to-broad transition for video person re-identification. In *Proceedings of the IEEE/CVF Conference on Computer Vision and Pattern Recognition*, pages 7339–7348, 2022. [2](#), [3](#), [6](#), [7](#)
- [2] Zechen Bai, Zhigang Wang, Jian Wang, Di Hu, and Errui Ding. Unsupervised multi-source domain adaptation for person re-identification. In *Proceedings of the IEEE/CVF Conference on Computer Vision and Pattern Recognition*, pages 12914–12923, 2021. [2](#)
- [3] Slawomir Bak, Peter Carr, and Jean-Francois Lalonde. Domain adaptation through synthesis for unsupervised person re-identification. In *Proceedings of the European Conference on Computer Vision*, pages 189–205, 2018. [2](#)
- [4] Guangyi Chen, Yongming Rao, Jiwen Lu, and Jie Zhou. Temporal coherence or temporal motion: Which is more critical for video-based person re-identification? In *Proceedings of the European Conference on Computer Vision*, pages 660–676. Springer, 2020. [1](#)
- [5] Zhihao Chen, Lei Zhu, Liang Wan, Song Wang, Wei Feng, and Pheng-Ann Heng. A multi-task mean teacher for semi-supervised shadow detection. In *Proceedings of the IEEE/CVF Conference on Computer Vision and Pattern Recognition*, 2020. [4](#), [5](#)
- [6] Yoonki Cho, Woo Jae Kim, Seunghoon Hong, and Sung-Eui Yoon. Part-based pseudo label refinement for unsupervised person re-identification. In *Proceedings of the IEEE/CVF Conference on Computer Vision and Pattern Recognition*, pages 7308–7318, 2022. [2](#)
- [7] Chanho Eom, Geon Lee, Junghyup Lee, and Bumsub Ham. Video-based person re-identification with spatial and temporal memory networks. In *Proceedings of the IEEE/CVF International Conference on Computer Vision*, pages 12036–12045, 2021. [2](#)
- [8] Xinqian Gu, Hong Chang, Bingpeng Ma, Hongkai Zhang, and Xilin Chen. Appearance-preserving 3d convolution for video-based person re-identification. In *Proceedings of the European Conference on Computer Vision*, pages 228–243. Springer, 2020. [2](#), [6](#), [7](#)
- [9] Xinqian Gu, Hong Chang, Bingpeng Ma, Shutao Bai, Shiguang Shan, and Xilin Chen. Clothes-changing person re-identification with rgb modality only. In *Proceedings of the IEEE/CVF Conference on Computer Vision and Pattern Recognition*, pages 1060–1069, 2022. [2](#), [6](#), [7](#)
- [10] Jian Han, Ya-Li Li, and Shengjin Wang. Delving into probabilistic uncertainty for unsupervised domain adaptive person re-identification. In *Proceedings of the AAAI Conference on Artificial Intelligence*, pages 790–798, 2022. [2](#)
- [11] Martin Hirzer, Csaba Beleznai, Peter M Roth, and Horst Bischof. Person re-identification by descriptive and discriminative classification. In *Image Analysis: 17th Scandinavian Conference*, pages 91–102. Springer, 2011. [6](#)
- [12] Ruibing Hou, Hong Chang, Bingpeng Ma, Shiguang Shan, and Xilin Chen. Temporal complementary learning for video person re-identification. In *Proceedings of the European Conference on Computer Vision*, pages 388–405. Springer, 2020. [2](#), [6](#), [7](#)
- [13] Zhengdong Hu, Yifan Sun, Yi Yang, and Jianguang Zhou. Divide-and-regroup clustering for domain adaptive person re-identification. In *Proceedings of the AAAI Conference on Artificial Intelligence*, pages 980–988, 2022. [2](#)
- [14] Cuicui Kang. Is synthetic dataset reliable for benchmarking generalizable person re-identification? In *Proceedings of the IEEE International Joint Conference on Biometrics*, pages 1–8. IEEE, 2022. [3](#)
- [15] Diederik P Kingma and Jimmy Ba. Adam: A method for stochastic optimization. *arXiv preprint arXiv:1412.6980*, 2014. [5](#)
- [16] Wei Li, Rui Zhao, Tong Xiao, and Xiaogang Wang. Deep-reid: Deep filter pairing neural network for person re-identification. In *Proceedings of the IEEE Conference on Computer Vision and Pattern Recognition*, pages 152–159, 2014. [1](#)
- [17] Zongyi Li, Yuxuan Shi, Hefei Ling, Jiazhong Chen, Qian Wang, and Fengfan Zhou. Reliability exploration with self-ensemble learning for domain adaptive person re-identification. In *Proceedings of the AAAI Conference on Artificial Intelligence*, pages 1527–1535, 2022. [2](#)
- [18] Shengcai Liao and Ling Shao. Graph sampling based deep metric learning for generalizable person re-identification. In *Proceedings of the IEEE/CVF Conference on Computer Vision and Pattern Recognition*, pages 7359–7368, 2022. [6](#), [7](#)
- [19] Chih-Ting Liu, Jun-Cheng Chen, Chu-Song Chen, and Shao-Yi Chien. Video-based person re-identification without bells and whistles. In *Proceedings of the IEEE/CVF Conference on Computer Vision and Pattern Recognition*, pages 1491–1500, 2021. [2](#)
- [20] Xuehu Liu, Pingping Zhang, Chenyang Yu, Huchuan Lu, and Xiaoyun Yang. Watching you: Global-guided reciprocal learning for video-based person re-identification. In *Proceedings of the IEEE/CVF Conference on Computer Vision and Pattern Recognition*, pages 13334–13343, 2021. [2](#)
- [21] Deqiang Ouyang, Yonghui Zhang, and Jie Shao. Video-based person re-identification via spatio-temporal attentional and two-stream fusion convolutional networks. *Pattern Recognition Letters*, 117:153–160, 2019. [1](#)
- [22] Xiaoxiao Sun and Liang Zheng. Dissecting person re-identification from the viewpoint of viewpoint. In *Proceedings of the IEEE/CVF Conference on Computer Vision and Pattern Recognition*, 2019. [1](#), [3](#)
- [23] Likai Wang, Xiangqun Zhang, Ruize Han, Jialin Yang, Xiaoyu Li, Wei Feng, and Song Wang. A benchmark of video-based clothes-changing person re-identification. *arXiv preprint arXiv:2211.11165*, 2022. [3](#), [5](#), [6](#)
- [24] Taiqing Wang, Shaogang Gong, Xiatian Zhu, and Shengjin Wang. Person re-identification by video ranking. In *Proceedings of the European Conference on Computer Vision*, pages 688–703. Springer, 2014. [6](#)
- [25] Yingquan Wang, Pingping Zhang, Shang Gao, Xia Geng, Hu Lu, and Dong Wang. Pyramid spatial-temporal aggregation for video-based person re-identification. In *Proceedings*

- of the *IEEE/CVF International Conference on Computer Vision*, pages 12026–12035, 2021. 2, 6, 7
- [26] Yanan Wang, Xuezhi Liang, and Shengcai Liao. Cloning outfits from real-world images to 3d characters for generalizable person re-identification. In *Proceedings of the IEEE/CVF Conference on Computer Vision and Pattern Recognition*, pages 4900–4909, 2022. 3
- [27] Jinlin Wu, Lingxiao He, Wu Liu, Yang Yang, Zhen Lei, Tao Mei, and Stan Z Li. Cavit: Contextual alignment vision transformer for video object re-identification. In *Proceedings of the European Conference on Computer Vision*, pages 549–566. Springer, 2022. 2, 6, 7
- [28] Yuhang Wu, Tengteng Huang, Haotian Yao, Chi Zhang, Yuanjie Shao, Chuchu Han, Changxin Gao, and Nong Sang. Multi-centroid representation network for domain adaptive person re-id. In *Proceedings of the AAAI Conference on Artificial Intelligence*, pages 2750–2758, 2022. 2
- [29] Suncheng Xiang, Yuzhuo Fu, Guanjie You, and Ting Liu. Unsupervised domain adaptation through synthesis for person re-identification. In *Proceedings of the IEEE International Conference on Multimedia and Expo*, pages 1–6. IEEE, 2020. 3
- [30] Suncheng Xiang, Guanjie You, Leqi Li, Mengyuan Guan, Ting Liu, Dahong Qian, and Yuzhuo Fu. Rethinking illumination for person re-identification: A unified view. In *Proceedings of the IEEE/CVF Conference on Computer Vision and Pattern Recognition*, pages 4731–4739, 2022. 3
- [31] Jinjie You, Ancong Wu, Xiang Li, and Wei-Shi Zheng. Top-push video-based person re-identification. In *Proceedings of the IEEE/CVF Conference on Computer Vision and Pattern Recognition*, pages 1345–1353, 2016. 1
- [32] Hong-Xing Yu, Wei-Shi Zheng, Ancong Wu, Xiaowei Guo, Shaogang Gong, and Jian-Huang Lai. Unsupervised person re-identification by soft multilabel learning. In *Proceedings of the IEEE/CVF Conference on Computer Vision and Pattern Recognition*, pages 2148–2157, 2019. 2
- [33] Yunpeng Zhai, Shijian Lu, Qixiang Ye, Xuebo Shan, Jie Chen, Rongrong Ji, and Yonghong Tian. Ad-cluster: Augmented discriminative clustering for domain adaptive person re-identification. In *Proceedings of the IEEE/CVF Conference on Computer Vision and Pattern Recognition*, pages 9021–9030, 2020. 2
- [34] Tianyu Zhang, Lingxi Xie, Longhui Wei, Zijie Zhuang, Yongfei Zhang, Bo Li, and Qi Tian. Unrealperson: An adaptive pipeline towards costless person re-identification. In *Proceedings of the IEEE/CVF Conference on Computer Vision and Pattern Recognition*, pages 11506–11515, 2021. 1, 3
- [35] Ziyuan Zhang, Luan Tran, Xi Yin, Yousef Atoum, Xiaoming Liu, Jian Wan, and Nanxin Wang. Gait recognition via disentangled representation learning. In *Proceedings of the IEEE/CVF Conference on Computer Vision and Pattern Recognition*, pages 4710–4719, 2019. 6
- [36] Kecheng Zheng, Wu Liu, Lingxiao He, Tao Mei, Jiebo Luo, and Zheng-Jun Zha. Group-aware label transfer for domain adaptive person re-identification. In *Proceedings of the IEEE/CVF Conference on Computer Vision and Pattern Recognition*, pages 5310–5319, 2021. 2, 6, 7
- [37] Liang Zheng, Liyue Shen, Lu Tian, Shengjin Wang, Jiahao Bu, and Qi Tian. Person re-identification meets image search. *arXiv preprint arXiv:1502.02171*, 2015. 1
- [38] Liang Zheng, Zhi Bie, Yifan Sun, Jingdong Wang, Chi Su, Shengjin Wang, and Qi Tian. Mars: A video benchmark for large-scale person re-identification. In *Proceedings of the European Conference on Computer Vision*, pages 868–884. Springer, 2016. 6
- [39] Yi Zheng, Shixiang Tang, Guolong Teng, Yixiao Ge, Kaijian Liu, Jing Qin, Donglian Qi, and Dapeng Chen. Online pseudo label generation by hierarchical cluster dynamics for adaptive person re-identification. In *Proceedings of the IEEE/CVF International Conference on Computer Vision*, pages 8371–8381, 2021. 2